An approach to evaluate internal friction angle from dynamic penetration tests

Une approche pour prédire l'angle de frottement interne de sols purement frottant à partir d'essais SPT

B.O. Lobo; F. Schnaid & M.M. Rocha
Federal University of Rio Grande do Sul, Brazil
E. Odebrecht
University of Santa Catarina State, Brazil

ABSTRACT

This paper presents an approach to predict the internal friction angle of cohesionless soils from dynamic penetration tests. The proposed methodology allies the dimensional equation technique (π numbers) with a numerical simulation routine that is able to reproduce the dynamic test response for a SPT or for any other dynamically driven device such as LPT (Lobo, 2007). The numerical routine models the dynamic reaction mechanism, predicting the SPT penetration or blow count N. Based on typical resistance and rigidity values of cohesionless soils, an analytical solution is proposed to assess the effective friction angle. The results have proven it possible to model the penetration mechanism and, as a consequence, to use a dynamic test as an inverse boundary value problem to assess soil properties in granular materials.

RÉSUMÉ

La communication présente une approche pour prédire l'angle de frottement interne de sols purement frottants à partir d'essais SPT. La méthode proposée combine la technique de l'analyse dimensionnelle (π numbers) et une procédure numérique pour reproduire la réponse dynamique d'un essai SPT, ou de tout autre essai dynamique tel que le LPT (Lobo, 2007). La procédure numérique modélise le mécanisme de pénétration, fournissant une prédiction pour la valeur du nombre N. Basée sur des valeurs typiques de la résistance et de la rigidité des sols sans cohésion, une solution analytique est développée pour la détermination de l'angle de frottement drainé. Les résultats montrent qu'il est possible de modéliser le mécanisme de pénétration et, par conséquence, d'utiliser un essai dynamique comme un outil d'analyse inverse pour la détermination des propriétés de sols granulaires.

Keywords : SPT, internal friction angle, energy concepts

1 INTRODUCTION

Dynamic penetration tests such as SPT and LPT have been used in several countries as the primary index test for site characterization. Although widely used, they are traditionally interpreted on the basis of empirical approaches that can produce inaccurate responses and unreliable soil properties dependent on test equipment and adopted procedures.

An alternative method of dynamic penetration tests interpretation was recently proposed by Odebrecht et al (2005) and Schnaid et al (2008) from which the energy delivered to the rod composition is used to calculate a dynamic force that represents the reaction of soil to the penetration of the SPT sampler (F_d). Lobo (2007) extended these concepts by developing a numerical model based on energy conservation, dynamic equilibrium, cavity expansion theory (Berezantzev, 1961) and dimensionless Smith's model able to the dynamic test response of dynamically driven devices. This paper explores these concepts through a numerical simulation (Lobo, 2007) that uses dimensional equation technique (π numbers) to develop an analytical solution to predict the internal friction angle of cohesionless soils.

2 DYNAMIC PENETRATION MODEL

The stress wave activity due to hammer impact on rod compositions is solved numerically by 1-D discrete element method, idealizing the SPT test components (hammer, rod and sampler) in a series of 100mm bars elements connected by nodes. Each node concentrates the mass (m) of one element and its interaction with the subsequent node is characterized by the rigidity (k) and damping (c). The rigidity (k) represents the elastic deformation, while energy losses due to wave propagation and sampler-soil interaction are represented by damping (c) and reaction force (F_d), respectively. A schematic illustration of this scheme is shown in Figure 1.

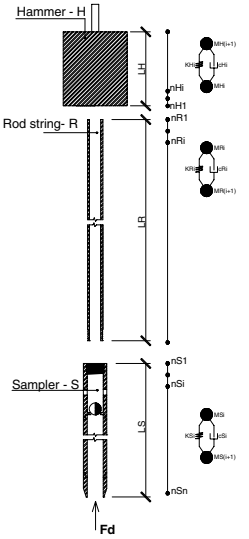

Figure 1. Model discretization schematic representation

doi:10.3233/978-1-60750-031-5-941

The model required input parameters are the geometrical characteristics of the driving tool: sectional area, length, drop height and blow efficiency. The sampler-soil interaction has its behavior modeled by the vertical effective stress (σ'_v), peak internal friction angle (ϕ') and small strain modulus (G_0).

The dynamic energy transferred from the hammer to the drill rods during penetration is modeled by the dynamic equilibrium principle:

$$m \cdot \ddot{u}(t) + c \cdot \dot{u}(t) = f(t) - k \cdot u(t) \quad (1)$$

where $\ddot{u}(t)$ represents the node acceleration, $\dot{u}(t)$ velocity, $u(t)$ displacement with time t and $f(t)$ the external applied force due to hammer impact load.

2.1 *The sampler-soil interaction*

When the stress wave arrives at the sampler tip, the soil-sampler interaction mechanism will produce a dynamic reaction force F_d. This reaction force is computed as the sum of three components:

$$F_d = F_{d,a} + F_{d,c} + F_{d,s} \quad (2)$$

where $F_{d,a}$, $F_{d,c}$ and $F_{d,s}$ are the sampler annulus, core and shaft dynamic reactions, respectively. These components are shown in Figure 2 together with the assumed load-deformation relationship for the soil during sampler penetration which is represented by the dimensionless Smith's model (Smith, 1960).

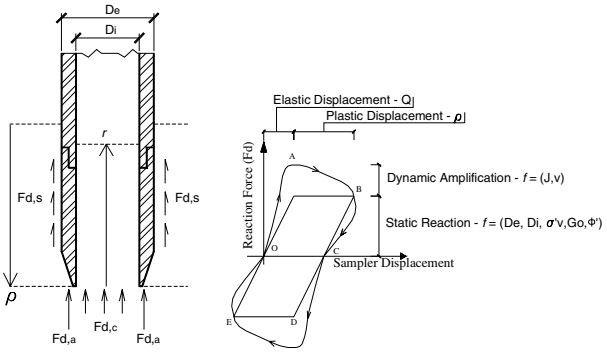

Figure 2. Sampler-soil interaction model

For each reaction mechanism, the load-unload behavior is defined by the ultimate static soil-resistance, F_u, the maximum elastic deformation (quake – Q), and an additional viscous resistance that represents the sampler-soil reaction amplification due to the dynamic loading (Smith, 1960; Coyle & Gibson, 1968). In the next three sections, a brief description of the theories used to compute the annular, core and shaft reaction component will be presented.

To properly define the stress changes due to the sampler penetration in the soil mass, two independent calibration procedures are required to assess both the static (F_u and *quake*) and the viscous dynamic responses represented by the Smith's damping (J). A detailed description of the calibration process presenting all simulated cases has been reported by Lobo (2007) and Lobo et al (2008).

2.1.1 *The annular reaction model*

The annular reaction load-unload cycle is represented by the diagram OABC of Figure 2 and computed by the equation (3):

$$F_{d,a} = K_a Q_a (1 + J_a V) \quad (3)$$

where K_a represents the static sampler-soil annular rigidity ($K_a = F_{u,a} / Q_a$), Q_a the annular maximum elastic displacement, J_a the annular Smith's damping and V the sampler penetration velocity. A value of J_a=0.5 s/m has been obtaind from comparisons between measured and simulated force velocity signals.

The static sampler-soil annulus reaction ($F_{u,a}$) is computed by:

$$F_{u,a} = A_a \cdot \sigma_u \quad (4)$$

where A_a represents the sampler effective cross section and σ_u the normal ultimate stress evaluated from the cavity expansion analysis:

$$\sigma_u = p'_o \cdot C_1 \cdot N_q \quad (5)$$

With p'_o being the mean effective stress, N_q the bearing capacity factor (Berezantzev et al, 1961) and C_1 a calibrated ultimate stress reduction factor equal to 0.75.

The maximum soil elastic displacement (Q_a) is computed by the pile´s displacement theory (Randolph & Wroth, 1978):

$$Q_a = \frac{F_{u,a}(1-\nu)}{2 \cdot G_o \cdot D_e} \eta \quad (6)$$

where D_e represents the sampler external diameter, ν the Poisson coefficient, η a depth factor to allow for the depth of sampler below ground surface (Randolph & Wroth, 1978) and G_o the soil small strain modulus. For this proposes, the depth factor (η) is adopted as a constant value equal to ½.

2.1.2 *The core reaction model*

The core reaction load-unload cycle is represented by the diagram OABC in Figure 2 and computed by equation (7):

$$F_{d,c} = K_c Q_c (1 + J_c V) \quad (7)$$

where K_c represents the static sampler-soil annular rigidity ($K_c = F_{u,c} / Q_c$), Q_c the core maximum elastic displacement, J_c the core Smith's damping and V the sampler penetration velocity. A J_c value equal to 0.15s/m has been obtained by calibration.

The static core reaction ($F_{u,c}$) is modeled as the core sectional area (A_c) times the mobilized core effective stress ($\sigma_{u,c}$), computed by the ratio of the internal soil column (ρ) and the normal ultimate stress (σ_u):

$$F_{u,c} = A_c \cdot \sigma_{u,c} \quad (8)$$

The mobilized core effective stress is computed by the ratio of the sampler plugging function (*DSP*) times the normal ultimate stress (σ_u). The DSP is the ratio between the internal soil column (ρ) and the maximum internal penetration (ρ_{plug}). The mobilized core effective stress increase (n) is defined as a quadratic function (n=2) by calibration procedures. Finally, the static core reaction is computed as:

$$F_{u,c} = A_c \cdot \left(\frac{\rho}{\rho_{plug}} \right)^n \cdot \sigma_{u,c} \quad (9)$$

The maximum soil elastic displacement (Q_c) is computed by an analogous solution adopted by the annular reaction given from Randolph & Wroth (1978) theory:

$$Q_a = \frac{F_{u,c}(1-\nu)}{2 \cdot G_o \cdot D_e} \eta \quad (10)$$

2.1.3 *The shaft reaction model*

The shaft reaction load-unload cycle is represented by the diagram OABCD of Figure 2 and computed by equation (3):

$$F_{d,s} = K_s Q_s (1 + J_s V) \quad (11)$$

where K_s represents the static sampler-soil annular rigidity ($K_s = F_{u,s} / Q_s$), Q_s the shaft maximum elastic displacement, J_s the shaft Smith's damping and V the sampler penetration velocity. A value of J_s = 0.15s/m was assumed from calibration.

The static friction reaction along the sampler external surface is computed by Coulomb failure criteria:

$$F_{u,s} = A_s \cdot \sigma'_{rf} \cdot \tan\delta_f = A_s \cdot K_s \cdot \sigma'_v \cdot \tan\delta_f \quad (12)$$

where σ'_{rf} is the radial effective stress and δ_f the interface friction angle at the sampler-soil interface. The radial effective stress is the product of in situ vertical effective stress, σ'_v, and the earth pressure coefficient, K_s. K_s has been assessed from calibration ($K_s = 0.25\ K_p$) and δf has been adopted as ($\delta_f = \phi' - 20°$).

The maximum elastic displacement for the shaft reaction (Q_s) is obtained from the pile solution for lateral displacement proposed by Randolph & Wroth (1978):

$$Q_s = \frac{\tau \cdot D_e}{G_o} \ln\left(\frac{r_m}{r_o}\right) \quad (13)$$

where r_m represents the radial distance when the shear stress become negligible (Randolph & Wroth, 1978).

3 INTERNAL FRICTION ANGLE

In this section, the dynamic penetration test routine was used to evaluate the variation of the SPT blow count for typical ground conditions (confining stresses and shear resistance values). Simulations are based on a safety hammer with blow efficiency of 60% and AW rod compositions. Two sets of parameters have been analyzed – varying either the vertical effective stress or the small shear strain modulus:

- Analysis 1: G_0 = 60MPa, σ'_v ranging from 30 to 300 kPa and ϕ' from 30 to 45°;
- Analysis 2: σ'_v =100kPa, G_0 ranging from 20 to 180MPa and ϕ' from 30 to 45°.

The concepts of dimensional equations (Buckingham's theorem) combined with the simulated average penetration per blow ($\Delta\rho$=0.3/N_{spt}) enables a physically consistent approach to evaluate the internal friction angle (ϕ') to be developed. For this proposes, two dimensionless parameters have been developed:

$$\Pi_1 = \frac{\Delta EPG}{\Delta\rho \cdot \sigma'_v \cdot D_e^2} \quad (14)$$

$$\Pi_2 = \phi' \quad (15)$$

where σ'_v is the vertical effective stress, D_e the sampler external diameter, $\Delta\rho$ the average sampler penetration per blow (300mm/N-SPT) and ΔEPG represents the energy delivered to the soil mass (Odebrecht, et al 2003; Schnaid, 2008).

$$\Delta EPG = \eta_3[\eta_1(H + \Delta\rho)M_h\ g + \eta_2(M_r\ g\ \Delta\rho)] \quad (16)$$

H being the hammer drop height, M_h the hammer mass, g the gravity acceleration, M_r the rod mass and η_1, η_2 and η_3 the efficiency coefficients used to account for energy losses (Odebrecht et al, 2005).

Analysis 1 allows the effects of confining stress for a given range of peak friction angles and the dimensionless parameter Π_1 (equation 14). Figure 3 shows the Π_1 sensitivity to vertical effective stress variation for a G_0 value of 60MPa. From this figure, a small variation of Π_1 with the confining stress is observed, leading to conclude that this dimensional equation incorporate the effects of confining stresses due to peak friction angle variation.

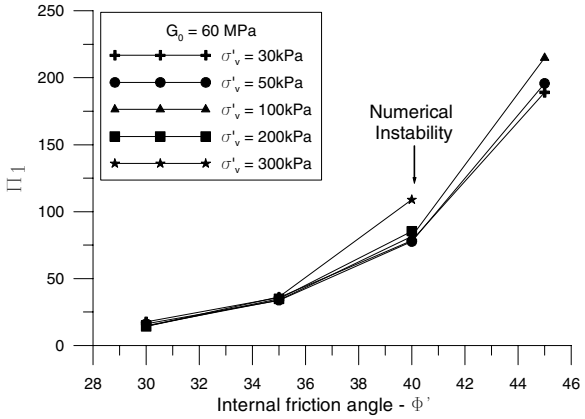

Figure 3. Π_1 variation with vertical effective stress

The simulated penetration per blow from Analysis 2 enables the effects of soil rigidity to be evaluated, for a range of given internal friction angles. The sensitivity of the dimensionless parameter Π_1 with soil rigidity is presented in Figure 4.

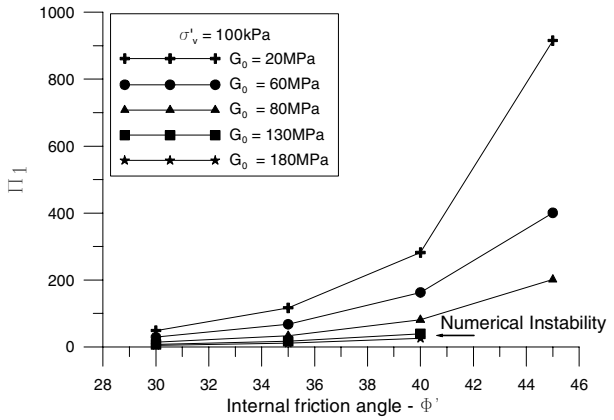

Figure 4. Π_1 variation with soil rigidity

Figure 4 shows that the dimensionless parameter Π_1 is fairly sensitive to soil rigidity. Thus a new dimensionless group was incorporated to equation (14) to isolate soil rigidity effects. A ratio between small strain modulus (G_0) and vertical effective stress (σ'_v) with an exponent "a" was selected for this propose.

$$\Pi_3 = \left(\frac{Go}{\sigma'_v}\right)^a \quad (17)$$

It was then possible to develop a new dimensionless paramter Π_{II} by multiplying Π_1 and Π_3

$$\Pi_{II} = \frac{\Delta EPG}{\Delta\rho \cdot \sigma'_v \cdot De^2}\left(\frac{Go}{\sigma'_v}\right)^a \quad (18)$$

The smallest sensitivity of Π_{II} with soil rigidity is obtained for an exponent a= -1/2. Figure 5 presents the variation of Π_{II} values with the internal friction angle, indicating rigidity effects have been isolated. The variation of the dimensionless parameter Π_{II} with the friction angle can be adjusted as an exponential function:

$$\Pi_{II} = \frac{1}{A} e^{\frac{1}{B}\phi'} \quad (19)$$

By combining equations (18) and (19) it is possible to assess the peak friction angle of cohesionless soils directly as:

$$\phi' = A \cdot \ln\left[B \frac{\Delta EPG}{\Delta\rho \cdot \sigma'_v \cdot De^2} \left(\frac{Go}{\sigma'_v} \right)^a \right] \quad (20)$$

where A and B are constants that represent the geometrical characteristics of a dynamic penetration device configuration. For the SPT, constants A and B can be assumed as 6.7 and 100, respectively.

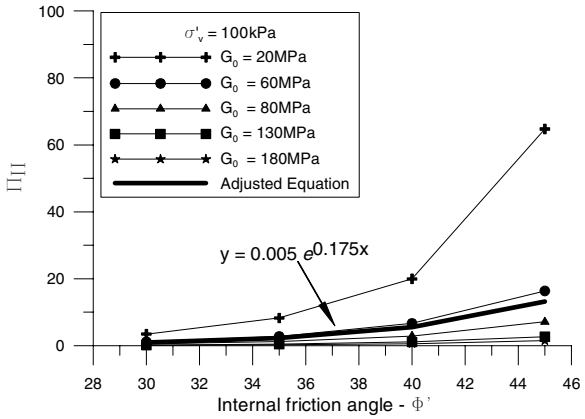

Figure 5. Π_{II} variation with the soil rigidity

4 VALIDATION

The validity of equation (20) can be made through a direct comparison with empirical solutions widely used in geotechnical practice. Two cases have been considered:

a) A cohesionless soil profile represented by a constant blow count (N-SPT) with depth. In the analysis, N_{60} is taken as 20 for vertical effective stress ranging from 30 to 300kPa;

b) A cohesionless Gibson soil profile, i.e. assuming SPT blow counts increasing linearly with depth. N_{60} values ranging from 7 to 34 and vertical effective stresses from 30 to 300kPa have been tested.

Figures 6 shows the set of predicted values of internal friction angles and compares these values to those obtained from the empirical correlations given by de Mello (1971), Bolton (1986) and Hatanaka & Uchida (1996). From these comparisons it is clear that the proposed methodology produces values within the same order of magnitude as the values derived from correlations currently used in engineering practice.

5 CONCLUSIONS

In this paper a rational numerically based methodology has been developed to evaluate the internal friction angle of cohesionless soils. The proposed methodology can be expressed by a simple equation capable of predicting ϕ' values in granular deposits by taking onto account the effect of soil rigidity. Although a general validation of the proposed approach from case based studies is still necessary before adopting this method in engineering design projects, the method proved to give consistent values of friction angle in a constant N profile as well as in a Gibson soil.

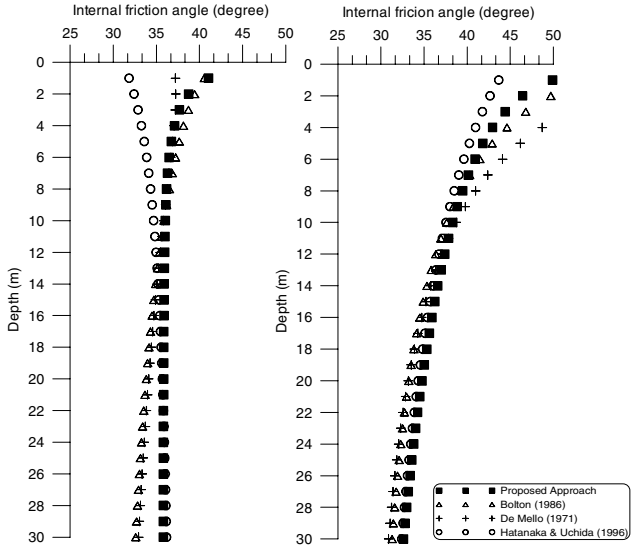

Figure 6. Internal friction angle prediction from SPT blow count: a) N profile increasing with depth (Gibson soil); b) N profile constant with depth

ACKNOWLEDGEMENTS

The authors are grateful to the *CAPES* and *CNPq* for the financial support of this research.

REFERENCES

Berezantzev, V.G., Khristoforov, V. & Golubkov, V. 1961. Load bearing capacity and deformation of piled foundations. Proc. 5th International Conference of Soil Mechanics and Foundation Engineering, Vol 2:11-15.

Bolton, M. D. (1986). The strength and dilatancy of sands. Geotechnique, vol. 36, no. 1: 65-78.

Coyle, H.M. & Gibson G. 1970. Empirical damping constants for sands and clays. Journal of Geotechnical Engineering 96 SM3, 949-965.

De Mello F.B.V 1971. The standard penetration test. In: IV Congresso Panamericano de Mecânica dos Solos e Engenharia de Fundações, v1: 1-86.

Hatanaka, M. & Uchida, A. (1996). Empirical correlation between penetration resistance and effective friction of sandy soil. Soils & Foundations, Vol. 36 (4): 1-9.

Lobo, B.O. 2007. Scale effects in the dynamic penetration process in soils. PhD. Qualification Exam. Federal Unversity of Rio Grande do Sul Civil Engenering Graduate – PPGEC-UFRGS (in portuguese).

Lobo, B.O., Schnaid, F. & Rocha, M.M. 2008. Numerical simulation of dynamic penetration tests. IV Congresso Luso-Brasileiro de Geotecnia.

Odebrecht, E., Schnaid, F. Rocha, M.M. & Bernardes, G. P. 2005. Energy efficiency for Standard Penetration Tests. Journal of Geotechnical Engineering 131 (10): 1252-1263.

Randolph, M. F. & Wroth, C. P. 1978. Analysis of deformation of vertically loaded piles. Journal of the geotechnical engineering division vol.104 no. GT12: 1465-1488.

Schnaid, F. Odebrecht O., Rocha M.M. & Bernardes G.P. 2008. Prediction of soil properties from the concepts of energy transfers in dynamic penetration tests. Journal of the geotechnical engineering division (in print).

Smith, E.A.L. 1960. Pile-driving analysis by the wave equation, Journal of the Soil Mechanics and Foundation Division – ASCE – vol. 86, no. SM4: 25-61.